Analysis of Precipitation Data Using Innovative Trend Pivot Analysis Method and Trend Polygon Star Concept: A Case Study of Soan River Basin, Potohar Pakistan

FIAZ HUSSAIN,[a] GOKMEN CERIBASI,[b] AHMET IYAD CEYHUNLU,[b] RAY-SHYAN WU,[c] MUHAMMAD JEHANZEB MASUD CHEEMA,[a] RANA SHAHZAD NOOR,[a] MUHAMMAD NAVEED ANJUM,[d] MUHAMMAD AZAM,[e] AND ARSLAN AFZAL[f]

[a] *Department of Agricultural Engineering, Pir Mehr Ali Shah Arid Arid Agriculture University Rawalpindi, Rawalpindi, Pakistan*
[b] *Department of Civil Engineering, Sakarya University of Applied Sciences, Sakarya, Turkey*
[c] *Department of Civil Engineering National Central University, Chung-Li, Taiwan*
[d] *Department of Land and Water Conservation Engineering, Pir Mehr Ali Shah Arid Arid Agriculture University Rawalpindi, Rawalpindi, Pakistan*
[e] *Department of Structure and Environmental Engineering, Pir Mehr Ali Shah Arid Arid Agriculture University Rawalpindi, Rawalpindi, Pakistan*
[f] *Department of Energy Systems Engineering, Pir Mehr Ali Shah Arid Arid Agriculture University Rawalpindi, Rawalpindi, Pakistan*

(Manuscript received 8 May 2022, in final form 8 September 2022)

ABSTRACT: The trend analysis approach is adopted for the prediction of future climatological behavior and climate change impact on agriculture, the environment, and water resources. In this study, the innovative trend pivot analysis method (ITPAM) and trend polygon star concept method were applied for precipitation trend detection at 11 stations located in the Soan River basin (SRB), Potohar region, Pakistan. Polygon graphics of total monthly precipitation data were created and trends length and slope were calculated separately for arithmetic mean and standard deviation. As a result, the innovative methods produced useful scientific information and helped in identifying, interpreting, and calculating monthly shifts under different trend behaviors, that is, increase in some stations and decrease in others of precipitation data. This increasing and decreasing variability emerges from climate change. The risk graphs of the total monthly precipitation and monthly polygonal trends appear to show changes in the trend of meteorological data in the Potohar region of Pakistan. The monsoonal rainfall of all stations shows a complex nature of behavior, and monthly distribution is uneven. There is a decreasing trend of rainfall in high land stations of SRB with a significant change between the first dataset and the second dataset in July and August. It was examined that monsoon rainfall is increasing in lowland stations indicating a shifting pattern of monsoonal rainfall from highland to lowland areas of SRB. The increasing and decreasing trends in different periods with evidence of seasonal variations may cause irregular behavior in the water resources and agricultural sectors.

SIGNIFICANCE STATEMENT: The monthly polygonal trends with risk graphs of total monthly precipitation data depicted a clear picture of climate change effects in the Potohar region of Pakistan. The monsoonal rainfall showed a significant decreasing trend in highland stations and an increasing trend in lowland stations, indicating a shifting pattern of monsoonal rainfall from highland to lowland areas.

KEYWORDS: Precipitation; Climate change; Time series; Climate variability; Trends

1. Introduction

The impacts of climate change are now, widespread, pervasive, intensifying, and unprecedented in thousands of years. According to the Intergovernmental Panel on Climate Change (IPCC) Sixth Assessment Report (AR6), it is unequivocal that human influence in terms of climate change has warmed the atmosphere, land, and ocean in multiple ways (IPCC 2021). It has thus been interpreted that Earth is in a state of climate emergency, and we should take necessary measures now and not wait for the end of this century to prevent or reduce its effects. Therefore, regional-scale approaches should be adopted to mitigate future possible changes in hydrometeorological variables such as runoff, rainfall, and temperature (Aktaş 2020). Trend analysis is one of the methodological approaches to predict and identify possible climate change impacts at small scales (Şen 2021). The purpose of trend analysis is to detect a change in observed time series data of rainfall, temperature, and so on to make future predictions. Trend identification, interpretations, and predictions are data processing approaches to detect and address visible and hidden issues in environmental changes such as climate change impacts on the water cycle.

The trend is the direction of the general tendency of time series data to increase (upward), decrease (downward), or

Denotes content that is immediately available upon publication as open access.

Supplemental information related to this paper is available at the Journals Online website: https://doi.org/10.1175/JAMC-D-22-0081.s1.

Corresponding author: Ray-Shyan Wu, raywu@ncu.edu.tw

DOI: 10.1175/JAMC-D-22-0081.1

remain stable (neutral). The linear or nonlinear temporal trend is the continuous and systematic increase or decrease of data along the time axis. The book *Innovative Trend Methodologies in Science and Engineering* by Z. Şen covers an innovative trend identification, detection, and analysis literature review. The book highlights the importance of time series analysis in many areas including water resources management. The innovative trend analysis techniques are objectively used to solve the issues of sustainable management logically and quantitatively (Şen 2017a). The trend analysis of natural, social, and artificial events is performed to identify systematic changes over at least 30 years of the dataset. It has been observed that, over the last 30 years, the number of trend studies and applications related to hydrometeorological time series as climate change has accelerated after Mann (1945) and Kendall's (1975) work known as the Mann–Kendall (MK) trend test—a classical approach. For example, trends have key implications for water resources planning and management in the future (IPCC 2007).

In the literature, there are numerous applications of the well-known MK test with the Theil–Sen approach (Theil 2011; Sen 1968) for the assessment of time series trend components and variability changes (Mann 1945; Sen 1968; Kendall 1975; Yu et al. 1993; Burn 1994; Bocheva et al. 2009; Kyselý 2009; Türkeş et al. 2009; Korhonen and Kuusisto 2010; Wilson et al. 2010; Tabari et al. 2011; Reihan et al. 2012; Hossain et al. 2014; Sayemuzzaman and Jha 2014; Hussain et al. 2015; Jones et al. 2015; Zhang et al. 2015; Swain et al. 2015; Bari et al. 2016; Chattopadhyay and Edwards 2016; Khatiwada et al. 2016; Birara et al. 2018; Chang et al. 2018; Güçlü 2018; Kabanda 2018; Nawaz et al. 2019; Phuong et al. 2019; Malik and Kumar 2020; Hussain et al. 2021) to name a few. Classical MK trend analysis with Sen's slope estimator approach has previously been used for identification of monotonic trend and statistical quantification of intercept and slope for a given time series. The drawbacks of the MK test are sample size, normality of the data, the serial independence of the given time series, prewhitening, and nonexistence of serial comparison among different sections of the same record and normal (Gaussian) probability distribution functions (pdf). The validity of MK trend test is possible under certain assumptions such as the length of data, independence of time series data, and its normal distribution. The other assumption is the calculation of trend slope magnitude through regression approach. In the past, hydrometeorological time series were assumed stationary stochastic process for climate change and trend detection purposes. Such assumption is no longer valid due to dynamic anthropogenic effects on climate, drainage basins, and atmosphere (Şen 2017b).

Trend analysis has been continuously on the research and application agenda, and scientific studies have shown the development of innovative methodologies and even modification of existing approaches for trend analysis. Methods such as Sen's innovation method, innovative trend analysis (ITA), innovative triangular trend analysis (ITTA), and innovative polygon trend analysis (IPTA) are the common trend analysis methods used in academic studies (Ceribasi et al. 2021a). Şen (2012, 2014) has presented ITA, a robust approach independent of sample size, nonnormality, and serial correlation. Innovative trend analysis easily interprets the visual inspection of trend type (increasing, decreasing, or no trend) and then calculate trend slope numerically. The ITA method uses Cartesian coordinate system and data on the 1:1 (45°) straight line corresponds to no trend, and any deviation from the 1:1 line represents trend existence. This nonparametric ITA approach has been analyzed by many researchers in several scientific studies around the world (Sonali and Nagesh Kumar 2013; Şen 2014, 2017b; Dabanlı et al. 2016; Elouissi et al. 2016; Tabari et al. 2017; Wu and Qian 2017; Mohorji et al. 2017; Alashan 2018; Güçlü et al. 2018; Dabanlı and Şen 2018; Almazroui et al. 2019; Alifujiang et al. 2020; Wang et al. 2020; Singh et al. 2021). Şen et al. (2019) introduced IPTA to explore trend possibilities in monthly hydrometeorological time series. IPTA is a nonparametric approach to identifying the trend and trend transitions between successive sections of the two equal segments from the original hydrometeorological time series leading to a 12-sided irregular trend polygon, which provides a productive basis for finer interpretation with linguistic and numerical interpretations and inferences from a given time series. This method is free from assumptions and can be applied directly. In the literature, few studies used the IPTA method for the analysis of hydrometeorological time series data (Şen et al. 2019; Ceribasi et al. 2021b; Ceribasi and Ceyhunlu 2021; Şen 2021; Şan et al. 2021; Hırca et al. 2022; Ahmed et al. 2022; Achite et al. 2021; Akçay et al. 2022).

The innovative trend pivot analysis method (ITPAM) and the trend polygon star concept method are new trend tests, and in the literature there are only two studies that used both methods for the temperature and precipitation trend analysis (Ceribasi et al. 2021a,b). Şen (2021) proposed the trend polygon star concept method. Ceribasi et al. (2021b) analyzed monthly average temperature data of six stations in the Susurluk Basin, Turkey, for 22 years (1996–2017) with innovative polygon trend analysis and trend polygon star concept methods. Polygon graphics were created for each station. The ITPAM determines risk classes by establishing a relationship between data (Ceribasi et al. 2021a). Ceribasi et al. (2021a) analyzed Susurluk Basin's total monthly precipitation data (2006–17) using ITPAM and determined the degree of trend risk. In the present study, the same methodology of ITPAM and the trend polygon star concept method has been applied to analyze Soan River basin (SRB) total monthly rainfall data to further strengthen the adaptability and applicability of both newest methods in academia research. Hussain et al. (2021) analyzed the temporal trends of rainfall data using the MK trend test in the selected study area of SRB in the Potohar region of Pakistan, and in the present study, we further want to analyze the degree of trend risk using ITPAM.

According to our understanding, all the parametric and nonparametric methods of trend analysis establish a relationship between data and made definitions such as increasing, decreasing, low, medium, and high, while ITPAM categorizes the risk classes showing changes between available datasets. ITPAM is a modified version of the IPTA method used to determine five risk classes of total monthly rainfall data of 11 stations of SRB. Moreover, the increasing and decreasing trend regions are

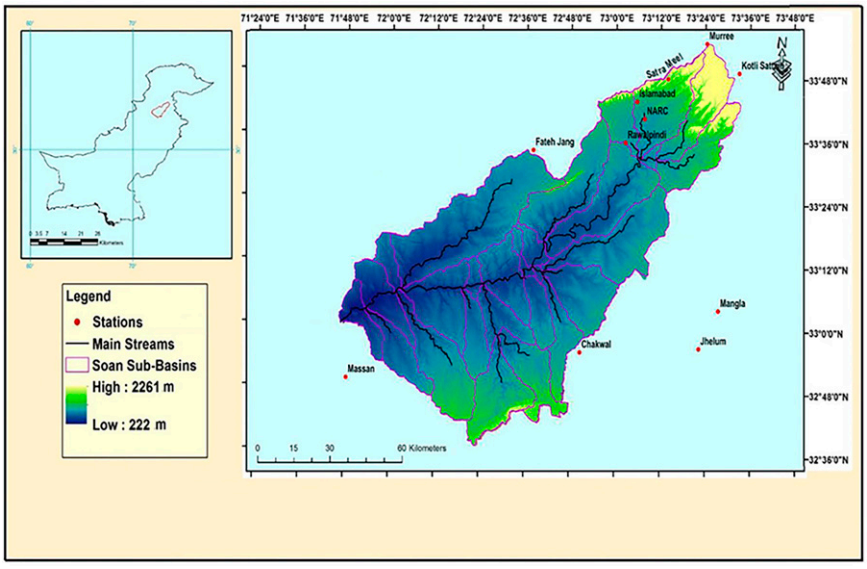

FIG. 1. Map of SRB, Pakistan: location of stations and elevation range.

divided into five classes for a clear understanding of this method. Furthermore, star graphs are generated using trend polygon star concept method to determine the transition distance from one month to another and the slopes of these transitions. The analysis is performed based on the arithmetic mean and standard deviation of rainfall data because the trend approach provides physical aspects of mean and standard deviation seasonal variations that are essential and refined parts hidden in holistic annual trend behaviors (Şen et al. 2019). Moreover, the analysis of hydrometeorological data based on the mean and standard deviation is very important for the effective planning of different human activities such as agricultural activities (irrigation practices, groundwater recharge), water supply, and hydroelectric power generation (Ceribasi et al. 2021a).

2. Materials and methods

a. Study area and data descriptions

SRB (Fig. 1) is the largest (9994 km^2) of six basins in the Potohar region within the elevation range of 222–2261 m above mean sea level. The climatic variation is from semiarid (central and southern part) to subhumid (northern part) in the study basin. Margalla and Murree hills surrounded the northern boundary of SRB, while the southern side is covered with a salt range (Hussain et al. 2021). The summer is hot (up to 31°C average temperature in June), whereas winter is relatively cold (mean temperature of 9°C in December). Mean annual rainfall ranges from 400 to 1710 mm in the plains areas to the mountainous terrain, respectively, and about two-thirds of the annual rainfall occurs during the monsoon period (June–September). The major crops are wheat, groundnut, chickpea, millets, sorghum, and fodders. Agriculture depends on the rainfall and perennial flow storage in small dams and minidams (Nabi et al. 2020).

Based on the elevation range and locations of stations, Hussain et al. (2021) divided the SRB into three zones, that is, high land stations within 540–2025-m elevation consisting of Murree, Satra Meel, Kotli Sattain, Islamabad, National Agricultural Research Centre (NARC), and Rawalpindi. Middle-land stations within the 283–529-m elevation range consist of Fatehjang, Mangla, and Jhelum, while lowlands stations within 218–522-m elevation consist of Chakwal and Massan. There are four climatological seasons of a year: winter [December–February (DJF)], spring or premonsoon [March–May (MAM)], summer or monsoon [June–September (JJAS)], and autumn or postmonsoon [October–December (OND)]. The same seasonal classification has been adopted by Adnan and Ullah (2022), Hussain et al. (2021), Adnan et al. (2019), and Asmat et al. (2018). For the analysis of rainfall data using ITPAM and trend polygon star concept method, the historical monthly time series records of 11 stations over the different period according to data availability (Table 1) in SRB was collected from Pakistan Meteorological Department (PMD), NARC, Water and Power Development Authority (WAPDA) and Soil and Water Conservation Research Institute (SAWCRI) in Pakistan. These organizations are national-level government agencies that record climatological data using all the standard operating procedures (SOPs), that is, total precipitation for 24 h previous to 0800 of the day according to Pakistan standard time (PST). Detailed descriptions of the 11 stations, data availability, and source of data are presented in Table 1. The gaps in the data series were completed using the time-based interpolation method (monthly records were determined as the mean values of the same month for a period between ±2 years; Mitchell et al. 1966).

b. ITPAM

ITPAM (Ceribasi et al. 2021a) is an extended version of IPTA (Şen et al. 2019). This method divides the available data into two separate periods and compares these two periods with each other. For example, if the dataset is between 1991 and 2020 (30 yr), the dataset is divided into two different periods

TABLE 1. Description of the meteorological stations.

Stations	Lon	Lat	Alt (m)	Data range	Source of data
Murree	73°24′3.148″E	33°54′58.847″N	2025	(1995–2020)	PMD
Satra Meel	73°14′3.118″E	33°48′16.042″N	715	(1995–2020)	PMD
Kotli Sattain	73°32′39.24″E	33°49′18.942″N	1352	(1991–2016)	PMD
Islamabad	73°5′42.464″E	33°43′50.202″N	569	(1991–2016)	PMD
NARC	73°7′44.157″E	33°40′23.056″N	551	(1995–2020)	NARC
Rawalpindi	73°2′50.035″E	33°35′41.506″N	540	(1995–2020)	PMD
Mangla	73°28′6.65″E	33°3′54.357″N	283	(1995–2020)	PMD
Jhelum	73°22′30.283″E	32°56′40.575″N	287	(1995–2020)	PMD
Fathejhang	72°38′14.979″E	33°33′58.479″N	514	(1990–2015)	SAWCRI
Chakwal	72°51′14.452″E	32°55′48.639″N	522	(1991–2016)	SAWCRI
Massan	71°49′26.733″E	32°49′39.852″N	335	(1995–2020)	WAPDA

of 15 years, and they are compared with each other. In other words, the first dataset will consist of the data measured in the years 1991–2005, and the second dataset in the years 2006–20. In ITPAM, five classes are used to identify the increasing trend (IT) or decreasing trend (DT) regions as 1) very high degree (VHD), 2) high degree (HD), 3) medium degree (MD), 4) low degree (LD), and 5) very low degree (VLD). This classification is used to define the risk range by establishing a relationship between the data being analyzed as the very high-degree class represents the first-degree risky range and the very low-degree class represents the fifth-degree risky range. ITPAM is hypothetically explained in Fig. 2 based on monthly data.

Figure 2a represents the improved form of the IPTA graph, where the increasing and decreasing trend regions are divided into five classes. The point on the 1:1 line is known as the no trend class. A cartesian coordinate graph (Fig. 2a) is obtained by dividing the data length of both axes into three equal parts. Then these divided parts are combined with a 1:1 line.

Figure 2b graph is the main output of ITPAM, which is obtained by adopting the following methodology:

1) Divide the available dataset (about 30 yr) into two equal parts.
2) Place first-half data (old series) on the x axis and second-half data (recent series) on the y axis in the Cartesian coordinate system.
3) The x-axis and y-axis coordinate system should be divided into five equal parts according to the defined five classifications of increasing and decreasing trends and risk levels (from first-degree risky class to fifth-degree risky class).

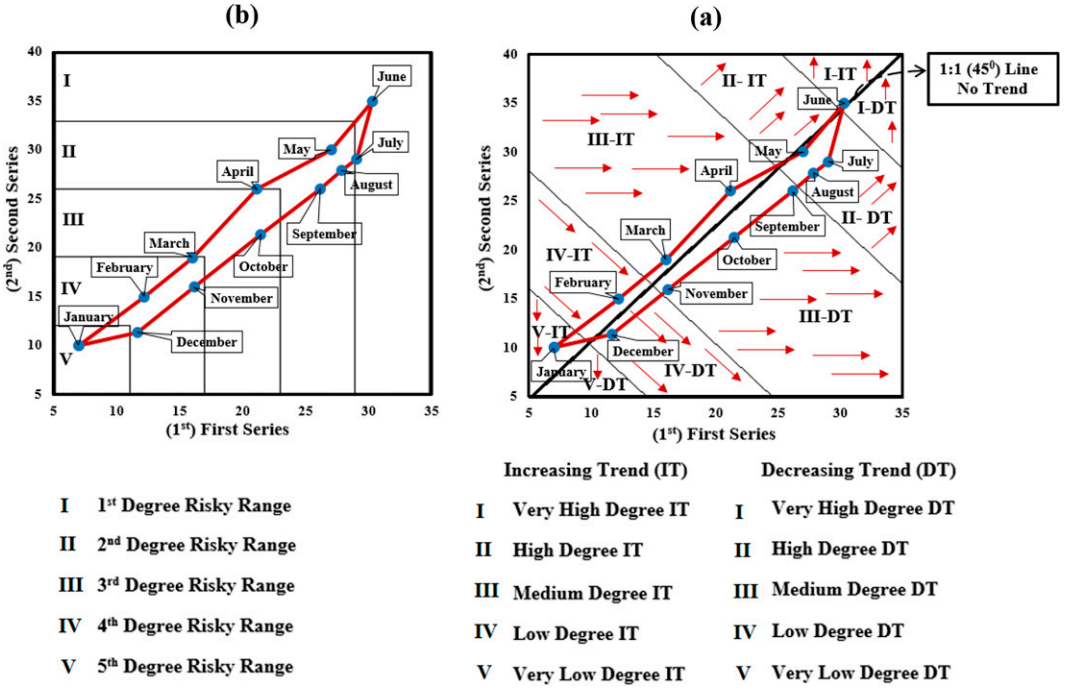

FIG. 2. Hypothetical ITPAM template for monthly data: (a) improved form of IPTA graph representing increasing and decreasing trend regions with degree classification; (b) ITPAM risky graph with classification.

TABLE 2. Explanation of hypothetical ITPAM analysis based on Fig. 2. DRC is "degree risky class." Trend regions and classes are defined in section 2b.

Months	Trend region	Trend class	Trend symbology	Risk class	Risk range
Jan	IT	VLD	↓	Fifth DRC	5–11
Feb		LD	↘	Fourth DRC	11–17
Mar		MD	→	Third DRC	17–23
Apr		MD	→	Second DRC	23–29
May	NT	HD	↗	Second DRC	23–29
Jun		VHD	↑	First DRC	29–35
Jul	DT	HD	↗	First DRC	29–35
Aug		HD	↗	Second DRC	23–29
Sep		MD	→	Second DRC	23–29
Oct		MD	→	Third DRC	17–23
Nov		MD	→	Fourth DRC	11–17
Dec		LD	↘	Fourth DRC	11–17

4) Read both graphs (Figs. 2a,b) in parallel and make it clear whether any point is risky in comparison with the other graph.
5) For a more clear understanding of ITPAM graphics, tabulation of extracted information is recommended as shown in Table 2. The information can be recorded as, for example, a monthly point in Fig. 1a is a medium-degree increasing trend whereas this point in Fig. 1b may be in the first-degree risky class. This position revealed considerable variation of this point between the first and second datasets.

Table 2 contains the information of Fig. 2 graphs, and it indicates that six months (July–December) show a decreasing trend. December showed a low-degree trend class as the fourth-degree risk class. The trend class of July and August is high degree, and the risk class is first and second degree, respectively. The trend class of September, October, and November is medium degree, while the risk class analysis indicated second-, third-, and fourth-degree risk class, respectively. May and June months lie on the 1:1 line and showed no trend. The other four months (January–April) show an increasing trend. January showed a very low-degree trend class and a fifth-degree risk class. The trend class of March and April is medium degree, while the risk class of these months is in the third- and second-degree risk class, respectively. February showed a high-degree increasing trend with fourth-degree risk class. The results considered in Table 2 indicated that some months are at a lower level in the ITPAM graph while showing the higher category in the risk graph. For instance, September, October, and November months show a medium-degree decreasing trend in the ITPAM graph, while their risk class is second, third, and fourth degree, respectively, as shown in the risk graph. This variation showed significant change between the first and second datasets for these months.

c. *Trend polygon star concept*

The trend polygon star concept (Şen 2021) illustrates the distance between two successive months, which reflects the temporal duration and slope of a straight-line trend. The corresponding trend polygon star concept of Fig. 2 is presented in Fig. 3, where the graph area is divided into four regions. The x axis represents the first half of the dataset, and the y axis indicates the second half of the dataset. All arrows originate from the point of origin (0,0). We can extract the following information from the trend star graph (Ceribasi et al. 2021b; Şen 2021):

1) The arrows show the transition between two months. The length of each arrow provides the amount of dataset for a respective month based on the trend polygon side extent from one month to the next. The largest arrow length represents the greatest transition between two months.

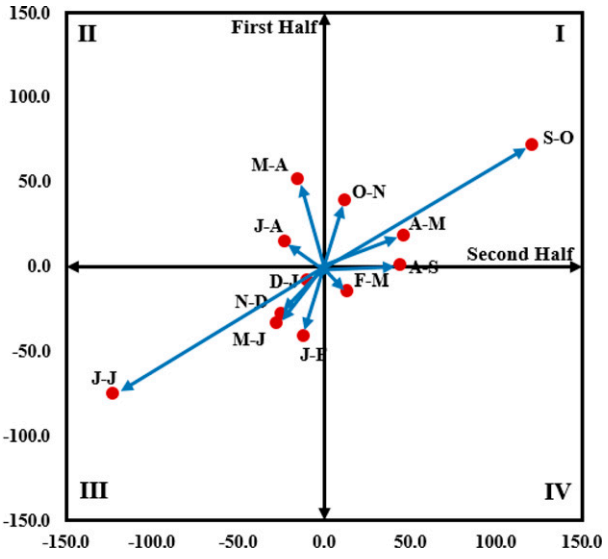

FIG. 3. Hypothetical trend polygon star concepts for monthly data, where in region I three corresponding months (A-M: April–May; S-O: September–October; O-N: October–November) showed an increasing trend and in region III five corresponding months (J-F: January–February; M-J: May–June; J-J: June–July; N-D: November–December; D-J: December–January) represent decreasing trends between both axes of dataset. The months in region II (J-A: July–August and M-A: March–April) represent an increase in the first half time duration. The months in region IV (F-M: February–March and A-S: August–September) represent a decrease in the second half time duration.

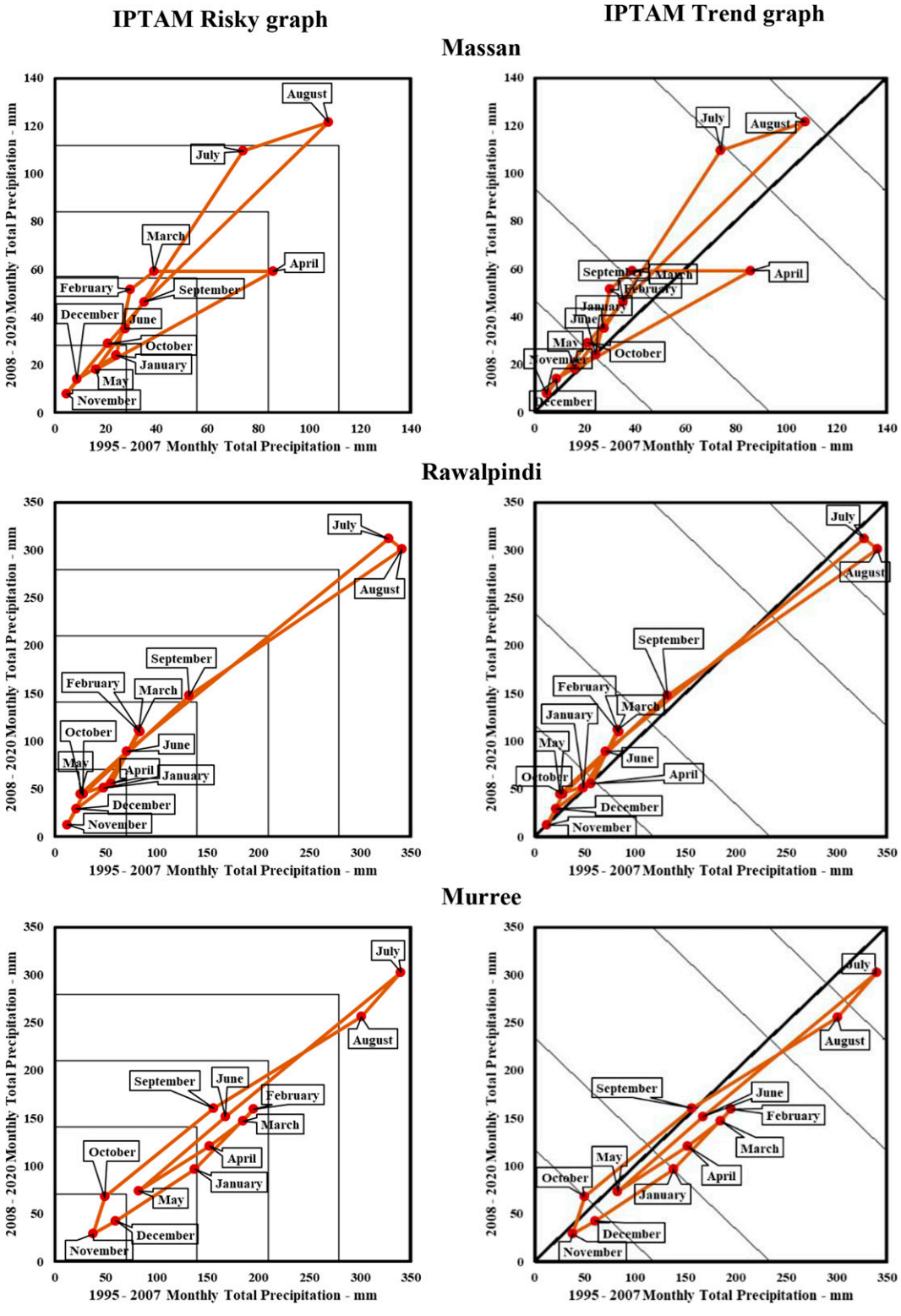

FIG. 4. ITPAM analysis results of monthly rainfall data based on the arithmetic mean parameter for each station of SRB.

2) The horizontal and vertical axis values correspond to the amount of monthly change during the first half and second half, respectively. The difference between the horizontal and vertical values reflects the monthly climate change.
3) Region I represents that both projections are positive, which represents an increasing trend in the first and second halves in both axes. Region III represents that both projections are negative, which represents a decreasing trend in the first and second halves in both axes.
4) The arrow direction in region II indicates an increase in the first-half time duration. The arrow direction in region IV indicates a decrease in the second-half time duration.
5) The slope of polygon is the ratio of vertical to horizontal projection.

3. Results

In this study, innovative trends methods (ITPAM and trend polygon star concept) were applied to total monthly precipitation data of SRB, Potohar region, Pakistan. The analysis has been performed based on the arithmetic mean data and standard deviation statistical parameters.

The arithmetic mean analysis results of monthly rainfall data for three stations (Murree, Rawalpindi, and Massan) are shown in Fig. 4, while other stations are given in Fig. S4 in the online supplemental material. Arithmetic mean analysis results are summarized in Table 3 for each station of Fig. S4, and the following findings were extracted.

Rainfall and its distribution are the most important climatic variable in this rainfed study area of the Potohar region because agriculture depends upon rainfall occurrence, which is the only source of available water for cropping. According to ITPAM analysis, it was observed that all the station's rainfall showed significant changes (increase or decrease) in July and August with the first degree of risk class. The results of rainfall data using ITPAM (supplemental Fig. S4; Table 3) indicated that July and August are in the first-degree risk group for all stations, and a significant change is observed between the first dataset and second dataset.

All stations' rainfall in August showed decreasing trend, with high to a very high-degree trend class. There is a significant change between the first and second dataset in August due to the indication of first-degree risk class. Besides, July is also in the first-degree risk group but shows decreasing rainfall trend in high land stations (Murree, Satrameel, NARC, Islamabad, and Rawalpindi), while other lowland stations (Massan, Chakwal, Fathejhang, and Mangla) show increasing rainfall trend in July, with a significant change in the first dataset and second data. Similarly, these low land stations are also showing an increasing rainfall trend in September month while high land stations showed decreasing trend. According to this examination, it was analyzed that for the months (June, July, August, and September) of the monsoon season, there is a decreasing trend of rainfall in high land stations of Soan River basin with a significant change between the first dataset and second dataset in July and August. It was also examined that monsoon rainfall is increasing in lowland stations indicating a shifting pattern of monsoonal rainfall from highland to lowland areas of the Soan River basin.

The November, December, and February months of the winter season show an increasing trend of rainfall, except for Murree and NARC station, but the change is not significant. Winter wheat is a major crop in this area, and timely rainfall is important for moisture availability and maximum yield. The sowing time of the wheat crop in the Potohar region is from mid-October to mid-November, and according to ITPAM analysis, October and November rainfall is increasing, indicating the availability of moisture at the sowing time of the wheat crop. At the time of sowing in January, there is a decreasing trend of rainfall, which may adversely affect wheat crop growth, while the increasing trend of rainfall in February and March months at the time of heading and flowering of wheat crop indicates a positive sign on the growth. The decreasing pattern of rainfall in April and increasing pattern in May at the time of wheat crop maturity and harvesting negatively affect crop growth and ultimately reduce the yield. These shifting patterns of monthly rainfall in the winter season indicate that there is a need for updating the cropping calendar according to rainfall water availability.

On the basis of the standard deviation analysis results (Fig. 5, along with Fig. S5 in the online supplemental material; Table 4), a significant change is observed between the first dataset and the second dataset of July and August at many stations. It was analyzed that most of the points have a high-degree trend class in the ITPAM graph with a first-degree risk class in the risk graph. Almost all stations of the Soan River basin showed an increasing trend of rainfall in February except Murree. July shows a significant decreasing rainfall trend except for Murree, NARC, Fathejhang, and Massan stations.

1) The results of rainfall data using ITPAM indicated that the July and August months of all stations are in the first-degree risk group, and a significant change is observed between the first dataset and second dataset.
2) Monsoonal months' (JJAS) rainfall of all stations shows a complex nature of behavior, and monthly distribution is uneven. June is showing an increasing trend of rainfall except for Murree station. The nonsignificant increasing trend of June rainfall relatively changed into a significant decreasing trend in July in most stations such as Jhelum, Mangla, Rawalpindi, Islamabad, Satrameel, and Kotli Sattain. June rainfall of Murree station shows a decreasing trend and shift into an increasing trend in July with first-degree risk class. It was also analyzed that the increasing trend of rainfall in July is shifting toward decreasing trend in August and September with first-degree risk class in other stations such as Massan and Chakwal. The rainfall in Rawalpindi and Islamabad indicated decreasing trend, with a significant change between the first dataset and second dataset in July, and changed into a nonsignificant increasing trend in August.
3) According to this examination, it was analyzed that for the months of the monsoon season (JJAS), there is a decreasing trend of rainfall in high land stations of Soan

TABLE 3. Evaluation of arithmetic mean analysis results of rainfall data of each station in the SRB.

Stations	Jan	Feb	Mar	Apr	May	Jun	Jul	Aug	Sep	Oct	Nov	Dec
Massan												
Trend (region-class)	IT-LD	IT-LD	IT-MD	DT-MD	IT-VLD	IT-LD	IT-MD	IT-HD	IT-LD	IT-LD	IT-VLD	IT-VLD
Trend symbol	↘	↘	→	→	↓	↘	→	↗	↘	↘	↓	↓
Risk class	Fifth DRC	Fourth DRC	Third DRC	Second DRC	Fifth DRC	Fourth DRC	Second DRC	First DRC	Fourth DRC	Fourth DRC	Fifth DRC	Fifth DRC
Chakwal												
Trend (region-class)	DT-VLD	IT-LD	IT-LD	DT-LD	IT-VLD	NT	IT-MD	DT-HD	DT-MD	DT-VLD	NT	IT-VLD
Trend symbol	↓	↘	↘	↘	↓	—	→	↗	→	↓	—	↓
Risk class	Fifth DRC	Fourth DRC	Fourth DRC	Fourth DRC	Fifth DRC	Fourth DRC	Second DRC	First DRC	Third DRC	Fifth DRC	Fifth DRC	Fifth DRC
Fathejhang												
Trend (region-class)	DT-VLD	IT-LD	DT-LD	DT-LD	DT-VLD	IT-LD	IT-HD	DT-VHD	DT-LD	DT-VLD	IT-VLD	DT-VLD
Trend symbol	↓	↘	↘	↘	↓	↘	↗	↑	↘	↓	↓	↓
Risk class	Fifth DRC	Fourth DRC	Fourth DRC	Fourth DRC	Fifth DRC	Fourth DRC	First DRC	First DRC	Fourth DRC	Fifth DRC	Fifth DRC	Fifth DRC
Jhelum												
Trend (region-class)	NT	NT	NT	NT	IT-VLD	IT-VLD	DT-HD	DT-HD	NT	NT	NT	IT-VLD
Trend symbol	—	—	—	—	↓	↓	↗	↗	—	—	—	↓
Risk class	Fifth DRC	Fourth DRC	Fourth DRC	Fifth DRC	Fifth DRC	Fourth DRC	First DRC	First DRC	Fourth DRC	Fifth DRC	Fifth DRC	Fifth DRC
Mangla												
Trend (region-class)	NT	IT-LD	IT-LD	IT-VLD	IT-VLD	IT-LD	IT-VHD	DT-VHD	IT-MD	NT	NT	NT
Trend symbol	—	↘	↘	↓	↓	↘	↑	↑	→	—	—	—
Risk class	Fifth DRC	Fourth DRC	Fourth DRC	Fifth DRC	Fifth DRC	Fourth DRC	First DRC	First DRC	Fourth DRC	Fifth DRC	Fifth DRC	Fifth DRC
Rawalpindi												
Trend (region-class)	NT	IT-LD	IT-LD	NT	IT-VLD	IT-VLD	DT-VHD	DT-VHD	IT-MD	IT-VLD	NT	IT-VLD
Trend symbol	—	↘	↘	—	↓	↓	↑	↑	→	↓	—	↓
Risk class	Fifth DRC	Fourth DRC	Fourth DRC	Fifth DRC	Fifth DRC	Fourth DRC	First DRC	First DRC	Second DRC	Fifth DRC	Fifth DRC	Fifth DRC
Islamabad												
Trend (region-class)	NT	IT-LD	IT-LD	NT	NT	IT-LD	DT-VHD	DT-HD	DT-MD	IT-VLD	NT	IT-VLD
Trend symbol	—	↘	↘	—	—	↘	↑	↗	→	↓	—	↓
Risk class	Fifth DRC	Fourth DRC	Fourth DRC	Fifth DRC	Fifth DRC	Fourth DRC	First DRC	First DRC	Fourth DRC	Fifth DRC	Fifth DRC	Fifth DRC
NARC												
Trend (region-class)	DT-VLD	DT-LD	DT-LD	DT-VLD	IT-VLD	IT-LD	DT-VHD	DT-HD	DT-MD	IT-VLD	IT-VLD	NT
Trend symbol	↓	↘	↘	↓	↓	↘	↑	↗	→	↓	↓	—
Risk class	Fifth DRC	Fourth DRC	Fourth DRC	Fifth DRC	Fifth DRC	Fourth DRC	First DRC	First DRC	Third DRC	Fifth DRC	Fifth DRC	Fifth DRC
Satra Meel												
Trend (region-class)	NT	IT-LD	IT-LD	DT-LD	IT-VLD	IT-LD	DT-VHD	DT-VHD	DT-MD	IT-VLD	NT	NT
Trend symbol	—	↘	↘	↘	↓	↘	↑	↑	→	↓	—	—
Risk class	Fifth DRC	Fourth DRC	Fourth DRC	Fifth DRC	Fifth DRC	Fourth DRC	First DRC	First DRC	Third DRC	Fifth DRC	Fifth DRC	Fifth DRC

TABLE 3. (*Continued*)

Stations	Jan	Feb	Mar	Apr	May	Jun	Jul	Aug	Sep	Oct	Nov	Dec
Murree												
Trend (region-class)	DT-LD	DT-MD	DT-MD	DT-MD	DT-LD	DT-MD	DT-VHD	DT-HD	NT	IT-LD	NT	DT-VLD
Trend symbol	↘	↑	↑	↑	↘	↑	↑	↗	—	↘	—	↓
Risk class	Fourth DRC	Third DRC	Third DRC	Third DRC	Fourth DRC	Third DRC	First DRC	First DRC	Third DRC	Fourth DRC	Fifth DRC	Fifth DRC
Kotli Sattian												
Trend (region-class)	NT	IT-LD	NT	NT	IT-VLD	NT	IT-VHD	DT-HD	IT-MD	IT-VLD	NT	IT-VLD
Trend symbol	—	—	↘	↑	—	—	—	—	—	↑	—	—
Risk class	Fourth DRC	Fourth DRC	Fourth DRC	Fourth DRC	Fourth DRC	Fourth DRC	First DRC	First DRC	Fourth DRC	Fifth DRC	Fifth DRC	Fifth DRC

River basin with a significant change between the first dataset and second dataset in July and August. It was also examined that monsoon rainfall is increasing in lowland stations, indicating a shifting pattern of monsoonal rainfall from highland to lowland areas of the Soan River basin.

4) December and January of the winter season are showing a decreasing trend of rainfall in high land stations, but the change is not significant.

Table 5 consists of statistical values of rainfall analyzed by the IPTA method in the Soan River basin. The maximum transition value between two months based on the arithmetic mean and standard deviation are shown in bold in Table 5. The transition is examined in terms of trend length and trend slope. For example, for the Rawalpindi station, the statistical results indicated that the maximum trend length is between June and July for arithmetic mean and standard deviation. The maximum trend slope shows that the arithmetic mean and the standard deviation is between March and April.

Trend polygon star concept method graphics of arithmetic mean and standard deviation analysis results of monthly rainfall data of three stations (Murree, Rawalpindi, and Massan) are given in Fig. 6 while other stations are given in Fig. S6 in the online supplemental material. It is examined that most of the station arrow's directions are in I and III based on the arithmetic mean parameter, showing the transition between both consecutive months for all stations. With the examination of Fig. S6, the following information emerges:

1) The highest transition was observed in August–September (A-S; highly increasing) and June–July (J-J; highly decreasing) between two months in all the stations based on the arithmetic mean. In the case of standard deviation, J-J is showing the highest transition in most of the stations.
2) For all stations, the arithmetic mean arrows showing transitions between four months (D-J, J-F, M-J, and J-J) are in region III (decreasing trend). Arrows showing transitions between other months (M-A, A-M, A-S, S-O, and O-N) are in region I (increasing trend).
3) The arrows of standard deviation indicating the transition between both months are in the first three regions. Arrow direction in region II (IV) represents an increase (decrease) in the first (second) half time duration, and the longest arrow indicates the highest transition.

Statistical values for 11 stations of the trend polygon star concept method are given in Table 6. The bold values show the maximum transition between two months. For example, for the Rawalpindi station, the statistical results show maximum horizontal is between June and July for arithmetic mean and standard deviation. June and July also showed maximum vertical for both standard deviation and arithmetic mean.

4. Discussion

Trend analysis is continuously acknowledged in research and application agendas due to the impact of climate change on the socioeconomic, environment, agriculture, and water

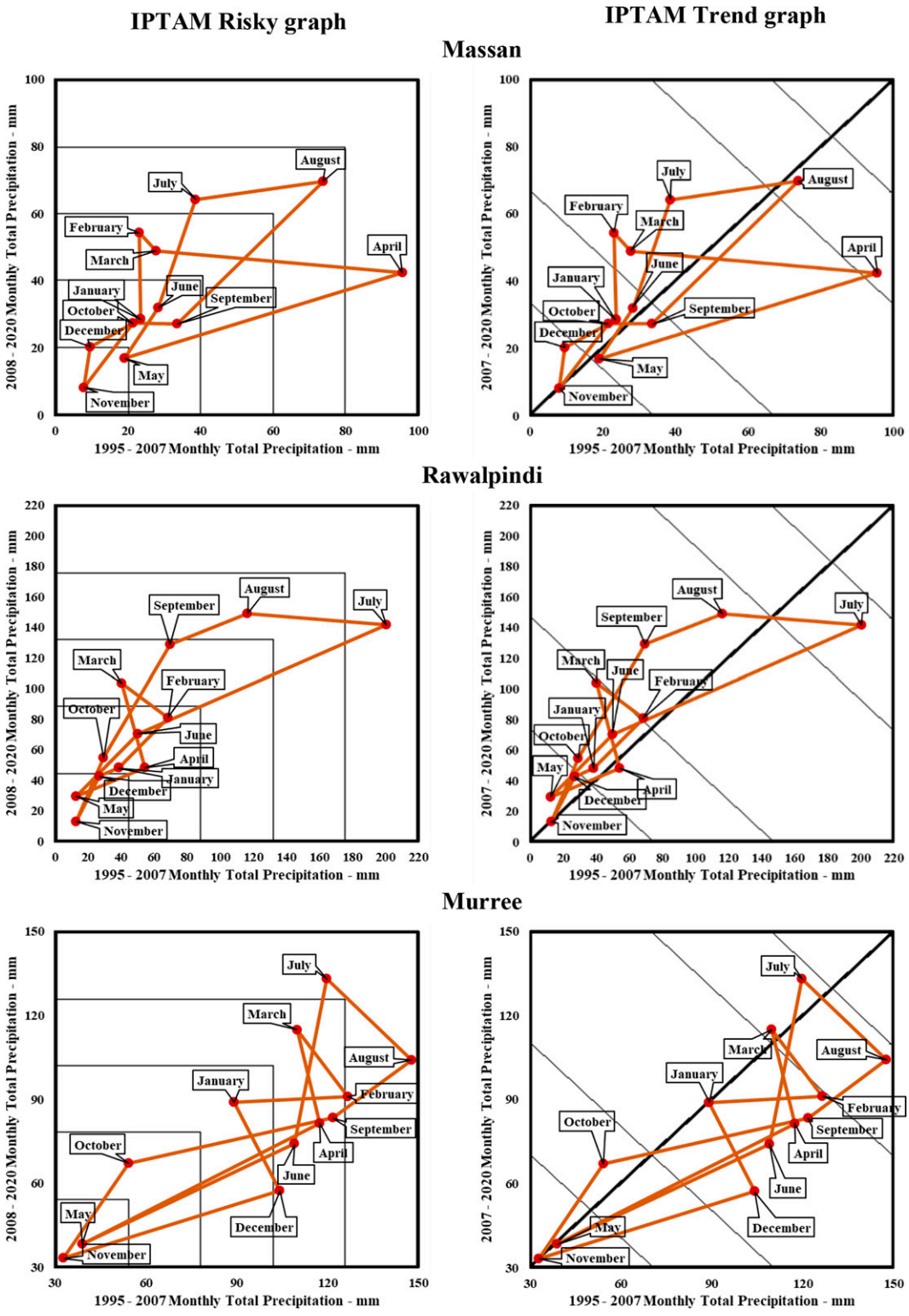

FIG. 5. As in Fig. 4, but based on standard deviation.

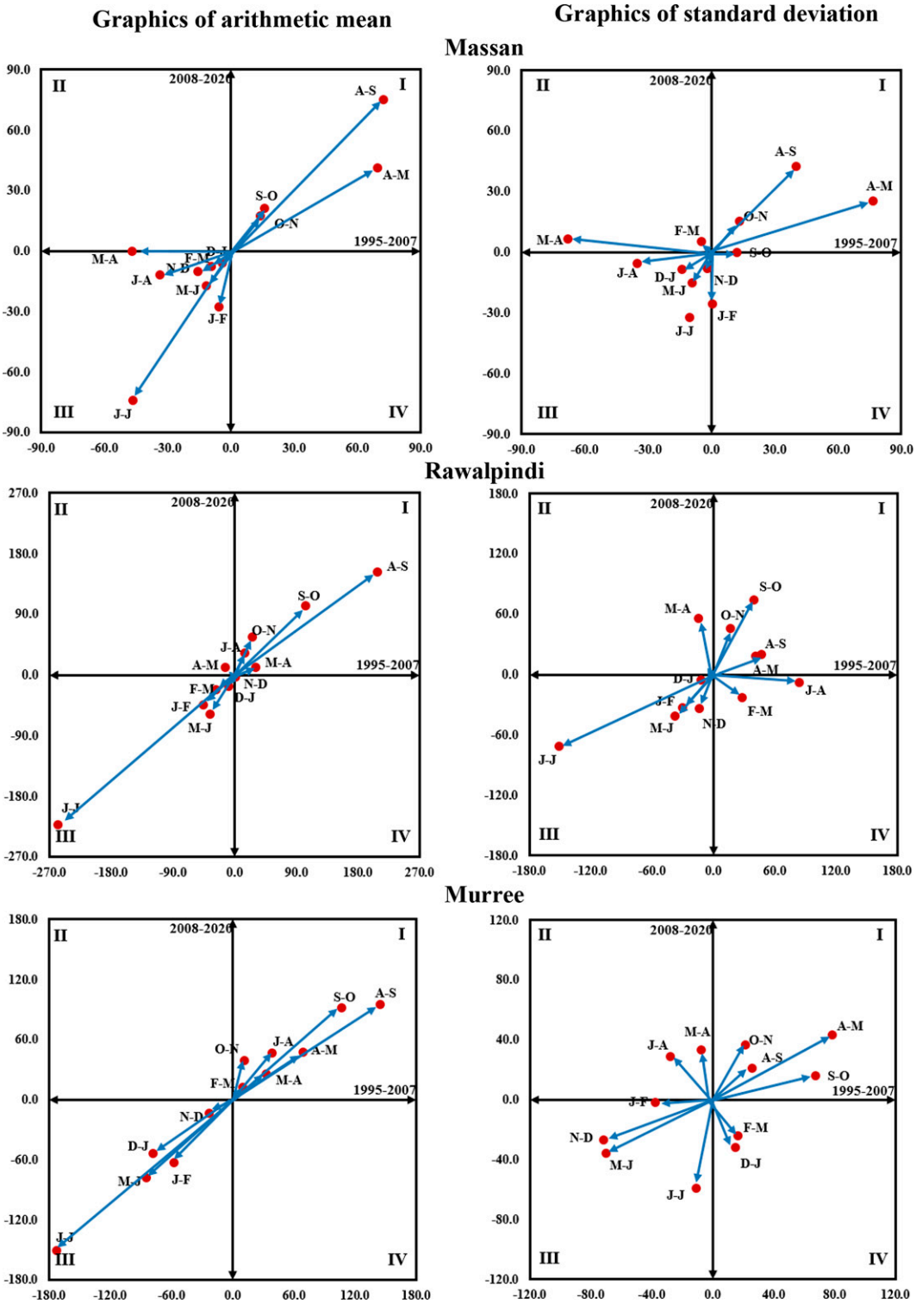

FIG. 6. Trend polygon star concept graphics of arithmetic mean and standard deviation analysis results of monthly rainfall data for each station of SRB.

TABLE 4. Evaluation analysis based on standard deviation of each rainfall station in the SRB.

Stations	Jan	Feb	Mar	Apr	May	Jun	Jul	Aug	Sep	Oct	Nov	Dec
Massan												
Trend (region-class)	IT-LD	IT-MD	IT-MD	DT-HD	DT-LD	IT-LD	IT-MD	DT-HD	DT-LD	IT-LD	NT	IT-VLD
Trend symbol	↘	→	→	↗	↘	↘	→	↗	↘	↘	—	↓
Risk class	Fourth DRC	Third DRC	Third DRC	First DRC	Fifth DRC	Fourth DRC	Second DRC	Second DRC	Fourth DRC	Fourth DRC	Fifth DRC	Fifth DRC
Chakwal												
Trend (region-class)	DT-MD	IT-MD	IT-MD	NT	NT	IT-MD	NT	DT-HD	DT-MD	DT-LD	NT	IT-VLD
Trend symbol	→	→	→	—	—	→	—	↗	→	↘	—	↓
Risk class	Third DRC	Third DRC	Second DRC	Fourth DRC	Fourth DRC	Second DRC	Third DRC	First DRC	First DRC	Fourth DRC	Fifth DRC	Fifth DRC
Fathejhang												
Trend (region-class)	DT-LD	IT-HD	DT-MD	NT	NT	IT-MD	IT-HD	IT-VHD	DT-MD	DT-LD	NT	DT-LD
Trend symbol	↘	↘	→	—	—	→	↗	↑	→	↘	—	↘
Risk class	Fourth DRC	First DRC	Third DRC	Third DRC	Fifth DRC	Second DRC	First DRC	First DRC	Third DRC	Fourth DRC	Fifth DRC	Fourth DRC
Jhelum												
Trend (region-class)	NT	DT-LD	NT	IT-LD	NT	IT-LD	DT-HD	DT-MD	IT-LD	DT-LD	NT	IT-VLD
Trend symbol	—	↘	—	↘	—	↘	↗	→	↘	↘	—	↓
Risk class	Fifth DRC	Fourth DRC	Fourth DRC	Fourth DRC	Fifth DRC	Fourth DRC	First DRC	Second DRC	Fourth DRC	Fourth DRC	Fifth DRC	Fifth DRC
Mangla												
Trend (region-class)	DT-LD	NT	IT-MD	IT-LD	IT-VLD	IT-LD	DT-HD	DT-HD	IT-MD	DT-LD	NT	IT-LD
Trend symbol	↘	—	→	↘	↓	↘	↗	↗	→	↘	—	↘
Risk class	Fourth DRC	Fourth DRC	Third DRC	Fourth DRC	Fourth DRC	Fourth DRC	First DRC	First DRC	Second DRC	Fourth DRC	Fifth DRC	Fourth DRC
Rawalpindi												
Trend (region-class)	IT-LD	IT-MD	IT-LD	DT-LD	IT-VLD	IT-LD	DT-HD	IT-MD	IT-MD	IT-LD	NT	IT-VLD
Trend symbol	↘	→	↘	↘	↓	↘	↗	→	→	↘	—	↓
Risk class	Fifth DRC	Fourth DRC	Third DRC	Fourth DRC	Fifth DRC	Fourth DRC	First DRC	Second DRC	Third DRC	Fourth DRC	Fifth DRC	Fifth DRC
Islamabad												
Trend (region-class)	DT-LD	NT	IT-LD	NT	NT	IT-LD	DT-HD	IT-MD	IT-MD	IT-VLD	NT	IT-VLD
Trend symbol	↘	—	↘	—	—	↘	↗	→	→	↓	—	↓
Risk class	Fifth DRC	Fourth DRC	Fourth DRC	Fifth DRC	Fifth DRC	Fourth DRC	First DRC	Third DRC	Third DRC	Fifth DRC	Fifth DRC	Fifth DRC
NARC												
Trend (region-class)	DT-LD	IT-LD	NT	DT-LD	IT-LD	IT-MD	IT-VHD	DT-HD	DT-MD	IT-VLD	NT	DT-LD
Trend symbol	↘	↘	—	↘	↘	→	↑	↗	→	↓	—	↘
Risk class	Fourth DRC	Fourth DRC	Fourth DRC	Fourth DRC	Third DRC	Third DRC	First DRC	First DRC	Third DRC	Fifth DRC	Fifth DRC	Fourth DRC

TABLE 4. (*Continued*)

Stations	Jan	Feb	Mar	Apr	May	Jun	Jul	Aug	Sep	Oct	Nov	Dec
Satra Meel												
Trend (region-class)	DT-LD	IT-MD	IT-MD	DT-LD	IT-VLD	IT-LD	DT-HD	DT-HD	DT-HD	IT-LD	NT	DT-LD
Trend symbol	↘	↑	→	↘	↓	↘	↗	↗	↗	↘	—	↗
Risk class	Fourth DRC	Third DRC	Third DRC	Fourth DRC	Fifth DRC	Fourth DRC	First DRC	First DRC	Second DRC	Fourth DRC	Fifth DRC	Fourth DRC
Murree												
Trend (region-class)	NT	DT-MD	IT-HD	DT-MD	NT	DT-MD	IT-HD	DT-HD	DT-MD	IT-LD	NT	DT-MD
Trend symbol	—	↑	↗	↑	—	↑	↗	↗	↑	↘	—	↑
Risk class	Third DRC	Second DRC	Second DRC	Second DRC	Fifth DRC	Second DRC	First DRC	First DRC	Second DRC	Fourth DRC	Fifth DRC	Second DRC
Kotli Sattian												
Trend (region-class)	DT-MD	DT-MD	IT-HD	IT-MD	IT-VLD	IT-LD	DT-HD	DT-MD	IT-MD	IT-VLD	NT	NT
Trend symbol	↑	↑	↗	↑	↓	↘	↗	→	↑	↓	—	—
Risk class	Fourth DRC	Third DRC	Second DRC	Fourth DRC	Fifth DRC	Third DRC	First DRC	Second DRC	First DRC	Fifth DRC	Fifth DRC	Fourth DRC

resources sectors. Innovation and modification in trend analysis has accelerated over the last 30 years. Şen (2012, 2014) has proposed an innovative trend analysis methodology and applied it in many scientific studies (Dabanlı et al. 2016; Elouissi et al. 2016; Tabari et al. 2017; Wu and Qian 2017; Mohorji et al. 2017; Alashan 2018; Güçlü et al. 2018; Dabanli and Şen 2018; Almazroui et al. 2019; Alifujiang et al. 2020; Wang et al. 2020; Singh et al. 2021). Şen et al. (2019) introduced IPTA, and Ceribasi et al. (2021a) introduced a modified version of IPTA called ITPAM. Şen (2021) proposed trend polygon star concept method. In the literature, few studies applied these new trend tests for the analysis of hydrometeorological data (Şen et al. 2019; Ceribasi et al. 2021a, b; Ceribasi and Ceyhunlu 2021; Şen 2021; Şan et al. 2021; Hırca et al. 2021; Ahmed et al. 2022; Achite et al. 2021). When previous studies were examined in the selected study area of SRB, Potohar region, Pakistan, no study was found in which hydrometeorological data were analyzed by applying innovative methods. Hussain et al. (2021) is the only study in which the monthly and annual temporal trends of rainfall data were analyzed using the MK trend test and Sen's slope estimator in the SRB, Potohar region, Pakistan. The comparison of the present study with Hussain et al. (2021) for the rainfall data series is given in Fig. 7. According to the comparison, the classical MK test provides information on increasing and decreasing trends while the newest test ITPAM also give no-trend information along with risk category and trend class. Hussain et al. (2021) found variations in monthly rainfall, that is, all stations showed a decrease in rainfall in December, and March with MK trend analysis while ITPAM analysis showed an increasing trend of rainfall in these months except in high land stations such as Murree and Satra Meel. MK test showed significant increasing and decreasing trends in June and August months, while ITPAM indicated in July and August months. Some stations in some months showed good agreement in trend detected with MK and ITPAM techniques, but the results obtained by ITPAM provide more information from a practical point of view, that is, indicate the monthly transition between the first and second dataset with a degree of risk to understand climatological behavior of study region. High land stations showed monsoonal rainfall shift in both trend test toward lowland station such as Murree to Massan stations, possibly due to their location. The high mountain stations such as Murree receive early onset of monsoon rainfall currents transported from Bay of Bengal later fall in northeast part deflected by Himalayas. Ali et al. (2020) also observed the monsoonal shift at Murree station from 1971 to 2010.

According to literature studies from the twentieth century, there is a shift in rainfall patterns at regional scales as well as on global scales due to global warming (Bradley et al. 1987; Maheras 1988; Diaz et al. 1989; Yu and Neil 1993; Rodriguez-Puebla et al. 1998). As for Pakistan's situation, precipitation indicated an increasing annual trend in the northern, northeastern, and northwestern regions (Ahmad et al. 2015; Ahmed et al. 2017) and a decreasing trend in the central and southern parts of the country (Hanif et al. 2013; Hussain and Lee 2014). The north and northwest coastal areas showed significant decreasing rainfall trends, whereas the southwest part and

TABLE 5. Statistical results of IPTA method of monthly rainfall data of each station in SRB.

Station	Jan–Feb	Feb–Mar	Mar–Apr	Apr–May	May–Jun	Jun–Jul	Jul–Aug	Aug–Sep	Sep–Oct	Oct–Nov	Nov–Dec	Dec–Jan
Massan												
Arithmetic mean												
Trend length (mm)	28.10	11.95	46.84	80.96	20.76	87.35	35.68	**104.20**	22.53	26.57	7.26	18.43
Trend slope	**4.93**	0.84	0.00	0.59	1.46	1.60	0.36	1.04	1.23	1.30	1.57	0.64
Std dev												
Trend length (mm)	25.74	7.22	68.08	**80.56**	17.74	33.78	35.55	58.39	12.13	20.31	8.30	16.24
Trend slope	**−47.37**	−1.16	−0.10	0.33	1.65	3.12	0.16	1.06	−0.01	1.12	4.80	0.60
Chakwal												
Arithmetic mean												
Trend length (mm)	45.77	6.13	18.34	22.25	64.84	77.51	68.11	**136.87**	66.38	23.73	2.14	32.16
Trend slope	2.19	**61.30**	4.23	0.44	0.91	1.10	−0.02	0.66	0.68	0.57	−1.08	0.51
Std dev												
Trend length (mm)	35.94	8.17	24.16	23.32	46.72	22.23	35.68	20.83	**54.06**	23.93	2.17	37.93
Trend slope	**5.41**	−0.12	4.45	1.18	3.19	−0.43	−0.07	2.33	0.25	0.41	−1.14	0.32
Fathejhang												
Arithmetic mean												
Trend length (mm)	63.61	44.25	22.50	46.14	71.35	188.60	47.68	**203.19**	76.34	22.56	20.57	15.46
Trend slope	1.47	−1.85	−0.35	0.75	3.46	0.90	−0.20	1.05	0.54	0.49	−0.01	**16.95**
Std dev												
Trend length (mm)	**68.78**	60.46	17.83	47.87	66.07	49.79	6.03	68.19	33.77	17.94	20.02	7.62
Trend slope	2.90	**−10.47**	−1.14	1.03	3.90	0.44	1.58	3.71	0.52	0.21	0.25	−2.94
Jhelum												
Arithmetic mean												
Trend length (mm)	26.16	4.26	23.88	22.29	58.30	**238.76**	31.20	212.41	77.29	21.13	9.65	33.74
Trend slope	0.77	−1.69	0.76	0.50	0.87	0.85	−2.38	0.68	1.01	0.97	**17.89**	0.72
Std dev												
Trend length (mm)	25.67	30.21	37.79	32.88	41.49	**127.42**	49.49	72.71	41.29	28.48	16.88	12.55
Trend slope	0.18	3.65	0.87	1.22	1.55	0.35	0.09	0.39	**−58.55**	0.46	3.09	0.67
Mangla												
Arithmetic mean												
Trend length (mm)	33.88	16.72	42.79	15.51	51.97	**216.52**	57.71	181.97	85.70	24.62	14.41	30.63
Trend slope	1.29	−1.51	2.16	−0.13	0.55	1.14	−1.37	0.61	1.10	1.06	**3.61**	0.68
Std dev												
Trend length (mm)	25.48	32.42	42.23	18.94	27.88	**102.03**	8.65	72.83	74.57	27.14	27.35	20.44
Trend slope	1.48	−2.35	3.82	0.44	0.42	0.35	0.90	−0.35	2.62	0.90	**4.28**	−0.21
Rawalpindi												
Arithmetic mean												
Trend length (mm)	68.22	2.63	61.97	32.62	63.46	**339.89**	16.80	258.76	146.33	35.88	19.00	34.86
Trend slope	1.64	−1.82	**2.10**	0.36	0.98	0.86	−0.83	0.73	0.99	2.10	1.92	0.81
Std dev												
Trend length (mm)	44.50	36.41	57.35	45.70	55.46	**166.44**	84.34	51.03	84.61	48.32	36.27	12.89
Trend slope	1.09	−0.80	**−3.93**	0.44	1.09	0.47	−0.09	0.42	1.85	2.77	2.41	0.47
Islamabad												
Arithmetic mean												
Trend length (mm)	62.89	5.12	55.23	31.94	60.30	**374.05**	28.40	242.08	164.90	36.28	25.56	40.96
Trend slope	1.58	0.30	1.54	1.17	1.27	0.78	1.24	0.72	0.83	2.17	**2.25**	0.57
Std dev												
Trend length (mm)	37.38	38.73	42.40	47.25	51.14	**244.46**	158.88	9.96	116.08	48.13	44.23	28.89
Trend slope	1.65	−0.67	**−5.43**	0.97	2.10	0.25	−0.04	1.11	0.91	2.87	2.23	−0.02

TABLE 5. (*Continued*)

Station	Jan–Feb	Feb–Mar	Mar–Apr	Apr–May	May–Jun	Jun–Jul	Jul–Aug	Aug–Sep	Sep–Oct	Oct–Nov	Nov–Dec	Dec–Jan
NARC												
Arithmetic mean												
Trend length (mm)	46.59	12.95	34.54	40.08	79.83	**288.59**	44.50	228.42	152.05	21.45	26.62	22.02
Trend slope	1.34	−1.78	1.33	−0.40	**2.13**	0.68	−1.71	1.03	0.34	1.44	0.53	0.41
Std dev												
Trend length (mm)	38.45	23.51	15.09	53.49	26.09	**134.16**	58.88	71.11	82.61	13.66	46.94	13.50
Trend slope	2.07	1.12	−2.23	−1.37	0.24	0.89	**−12.98**	0.71	0.65	0.76	0.49	0.97
Satra Meel												
Arithmetic mean												
Trend length (mm)	57.13	15.63	61.08	43.88	80.38	**343.41**	9.22	232.21	161.56	53.18	25.67	40.32
Trend slope	2.26	−0.22	1.88	0.40	1.27	0.83	**29.09**	0.87	0.79	1.58	0.80	1.00
Std dev												
Trend length (mm)	42.37	19.50	54.31	49.83	43.34	**143.71**	27.63	43.95	140.60	41.44	37.02	12.62
Trend slope	**3.38**	−1.08	−3.33	0.40	1.18	0.61	−0.65	0.02	0.59	3.27	1.09	0.83
Murree												
Arithmetic mean												
Trend length (mm)	85.05	16.05	42.08	83.82	115.02	**229.22**	60.89	173.18	141.02	40.99	26.12	94.68
Trend slope	1.09	1.24	0.78	0.68	0.92	0.88	1.20	0.66	0.86	**3.34**	0.59	0.70
Std dev												
Trend length (mm)	37.45	29.09	34.28	**89.43**	78.69	59.90	40.17	33.24	69.37	42.42	76.26	35.12
Trend slope	0.06	−1.43	−4.45	0.55	0.51	**5.52**	−1.04	0.80	0.24	1.71	0.37	−2.11
Kotli Sattian												
Arithmetic mean												
Trend length (mm)	45.12	23.45	68.48	37.14	67.91	**256.67**	94.98	172.77	117.41	19.15	19.33	58.74
Trend slope	1.17	0.60	0.98	0.60	0.69	1.12	**−441.00**	0.42	1.09	2.25	3.17	0.82
Std dev												
Trend length (mm)	24.60	50.31	58.61	41.99	39.35	**104.38**	45.13	48.36	99.61	15.10	33.64	22.73
Trend slope	−0.16	8.16	1.26	0.83	3.19	0.36	0.47	−1.30	2.42	**−81.08**	1.56	0.72

the plains areas have nonsignificant trends (Salma et al. 2012). Safdar et al. (2019) analyzed the northern Pakistan monsoonal rainfall and observed a significant decreasing trend (17.58 mm yr^{-1}) from 2010 to 2017. There is an adverse impact of climate change on the rainfall systems of Pakistan either by seasonal variations or by intensity modifications (Naheed et al. 2013). According to PMD, there has been a slow but steady spatial rainfall shift from the north to the west side. Similar findings indicate that the center of monsoon rains is Punjab, but the concentration of rainfall is moving slowly and steadily toward Khyber Puktonkhuwa (Chaudhry et al. 2009).

In this study, the results of two graphical methods (ITPAM and trend polygon star concept) represented the increasing and decreasing trends of rainfall in SRB, which indicated the impact of climatic change and shows there is a need to adopt an integrated approach to managing available water resources for agricultural practices. Moreover, these newest methods provided information on the degree of risk and trend class with the interpretation of monthly and seasonal shifts in climatological variable (precipitation) in terms of standard deviation and arithmetic mean graphs. These indicators are helpful tools for decision-makers to manage water resources in SRB.

5. Conclusions

The innovative trend pivot analysis method (ITPAM) and trend polygon star concept method were applied to total monthly rainfall data of 11 stations in Soan River basin (SRB), Potohar region, Pakistan. As a result of the study, ITPAM created two different graphs, that is, it developed the innovative polygonal trend analysis (IPTA) graph and the risk graph. The importance of the ITPAM and risk graphs was analyzed by the facts finding that a high class month in ITPAM graph was not first-degree risk graph. This finding indicated a significant change between the first and second datasets of that month, which represents the high risk factor in that month. It was also analyzed that some points in first category of risk class have a medium-degree trend in the risk and ITPAM graphs, respectively. This behavior represents the importance of ITPAM, which is used to manage many engineering applications such as water resources supply, irrigation practices, agricultural activities, and hydroelectric power generation. Moreover, trend lengths and trend slopes of rainfall data were calculated. The size of trend lengths and trend slopes show the variability between months. For example, using rainfall data for the Rawalpindi station, maximum trend lengths for the arithmetic mean and standard deviation are 339.89 and 166.44 mm, respectively, in June and July, while

TABLE 6. Statistical results of trend polygon star concept method of monthly rainfall data of each station in SRB.

Stations	Jan–Feb	Feb–Mar	Mar–Apr	Apr–May	May–Jun	Jun–Jul	Jul–Aug	Aug–Sep	Sep–Oct	Oct–Nov	Nov–Dec	Dec–Jan
Massan												
Arithmetic mean												
Horizontal (mm)	−5.58	−9.16	−46.84	69.71	−11.72	−46.19	−33.60	**72.36**	14.23	16.20	−3.90	−15.51
Vertical (mm)	−27.54	−7.67	−0.07	41.16	−17.14	−74.13	−12.02	**74.98**	17.47	21.06	−6.13	−9.97
Std dev												
Horizontal (mm)	0.54	−4.70	−67.76	**76.42**	−9.21	−10.32	−35.12	40.13	12.13	13.53	−1.69	−13.95
Vertical (mm)	−25.73	5.48	6.56	25.49	−15.16	−32.16	−5.50	**42.41**	−0.10	15.14	−8.12	−8.31
Chakwal												
Arithmetic mean												
Horizontal (mm)	−19.05	0.10	4.22	20.37	−48.01	−52.14	−68.09	**114.33**	54.91	20.58	1.45	−28.67
Vertical (mm)	−41.62	6.13	17.85	8.96	−43.58	−57.35	1.36	**75.25**	37.31	11.81	−1.57	−14.56
Std dev												
Horizontal (mm)	−6.54	8.11	5.29	15.08	−13.97	−20.44	−35.60	8.21	**52.43**	22.13	1.44	−36.15
Vertical (mm)	−35.34	−0.95	23.57	17.79	**−44.58**	8.75	2.47	19.14	13.17	9.11	−1.63	−11.48
Fathejhang												
Arithmetic mean												
Horizontal (mm)	−35.76	−21.05	21.24	36.83	−19.83	**−140.50**	−46.76	139.92	67.13	20.27	−20.57	−0.91
Vertical (mm)	−52.60	38.92	−7.42	27.80	−68.54	−125.81	9.31	**147.34**	36.36	9.91	0.18	−15.44
Std dev												
Horizontal (mm)	−22.45	−5.75	11.78	33.26	−16.40	**−45.51**	−3.22	17.76	29.95	17.56	−19.43	2.45
Vertical (mm)	−65.02	60.18	−13.39	34.42	−64.00	−20.20	−5.10	**65.83**	15.60	3.68	−4.81	−7.21
Jhelum												
Arithmetic mean												
Horizontal (mm)	−20.77	2.17	19.05	19.95	−43.94	**−181.75**	−12.08	175.75	54.39	15.21	−0.54	−27.45
Vertical (mm)	−15.90	−3.66	14.40	9.92	−38.32	**−154.84**	28.77	119.30	54.91	14.68	−9.63	−19.63
Std dev												
Horizontal (mm)	−25.25	−7.98	28.44	20.83	−22.49	**−120.22**	49.31	67.81	−0.71	25.91	−5.20	−10.44
Vertical (mm)	−4.63	−29.14	24.88	25.45	−34.87	**−42.23**	4.19	26.25	41.28	11.83	−16.06	−6.95
Mangla												
Arithmetic mean												
Horizontal (mm)	−20.77	9.23	18.00	15.38	−45.54	−143.08	−34.08	**155.31**	57.77	16.92	−3.85	−25.31
Vertical (mm)	−26.77	−13.95	38.82	−1.99	−25.05	**−162.52**	46.58	94.82	63.31	17.88	−13.88	−17.25
Std dev												
Horizontal (mm)	−14.24	12.67	10.69	17.37	−25.66	**−96.40**	6.42	68.67	26.56	20.17	−6.22	−20.02
Vertical (mm)	−21.13	−29.84	40.85	7.56	−10.89	−33.41	5.80	−24.28	**69.68**	18.16	−26.63	4.14
Rawalpindi												
Arithmetic mean												
Horizontal (mm)	−35.51	1.27	26.62	30.70	−45.36	**−257.14**	−12.92	208.57	104.24	15.44	−8.78	−27.12
Vertical (mm)	−58.25	−2.31	55.96	11.04	−44.38	**−222.27**	10.73	153.15	102.69	32.38	−16.85	−21.91
Std dev												
Horizontal (mm)	−30.11	28.36	−14.15	41.75	−37.43	**−150.52**	84.03	47.02	40.20	16.42	−13.93	−11.65
Vertical (mm)	−32.77	−22.83	55.58	18.58	−40.91	**−71.04**	−7.31	19.82	74.45	45.45	−33.49	−5.51
Islamabad												
Arithmetic mean												
Horizontal (mm)	−33.57	4.90	30.06	20.75	−37.24	**−295.55**	17.82	196.67	126.89	15.19	−10.38	−35.54
Vertical (mm)	−53.18	1.48	46.33	24.28	−47.43	**−229.26**	22.11	141.15	105.31	32.95	−23.35	−20.37
Std dev												
Horizontal (mm)	−19.34	32.14	−7.68	33.97	−21.98	**−237.08**	158.75	6.68	85.73	15.82	−18.11	−28.88
Vertical (mm)	−31.99	−21.62	41.70	32.85	−46.17	−59.60	−6.60	7.40	**78.27**	45.46	−40.35	0.67

TABLE 6. (*Continued*)

Stations	Jan–Feb	Feb–Mar	Mar–Apr	Apr–May	May–Jun	Jun–Jul	Jul–Aug	Aug–Sep	Sep–Oct	Oct–Nov	Nov–Dec	Dec–Jan
NARC												
Arithmetic mean												
Horizontal (mm)	−27.87	−6.33	20.74	37.22	−33.94	**−238.94**	−22.50	159.07	144.13	12.24	−23.48	−20.34
Vertical (mm)	−37.34	11.30	27.62	−14.87	−72.25	−161.82	38.39	**163.92**	48.43	17.62	−12.55	−8.44
Std dev												
Horizontal (mm)	−16.74	15.66	−6.18	31.56	−25.39	**−100.09**	−4.52	58.03	69.26	10.88	−42.17	9.71
Vertical (mm)	−34.61	17.53	13.77	−43.18	−5.99	**−89.35**	58.70	41.09	45.02	8.26	−20.62	9.37
Satra Meel												
Arithmetic mean												
Horizontal (mm)	−23.11	−15.28	28.66	40.76	−49.71	**−263.66**	0.32	175.28	126.83	28.43	−20.01	−28.50
Vertical (mm)	−52.25	3.32	53.94	16.23	−63.17	**−220.04**	9.22	152.31	100.08	44.94	−16.07	−28.51
Std dev												
Horizontal (mm)	−12.03	13.23	−15.63	46.24	−28.07	**−122.74**	−23.20	43.93	120.85	12.13	−24.97	−9.73
Vertical (mm)	−40.62	−14.33	52.01	18.58	−33.02	**−74.74**	15.00	1.00	71.86	39.63	−27.34	−8.03
Murree												
Arithmetic mean												
Horizontal (mm)	−57.37	10.08	33.18	69.16	−84.71	**−172.41**	38.99	144.62	106.88	11.76	−22.50	−77.70
Vertical (mm)	−62.79	12.49	25.88	47.36	−77.81	**−151.06**	46.77	95.28	91.99	39.27	−13.27	−54.11
Std dev												
Horizontal (mm)	−37.39	16.71	−7.52	**78.39**	−70.12	−10.68	−27.87	25.94	67.46	21.44	−71.42	15.07
Vertical (mm)	−2.06	−23.81	33.45	43.05	−35.70	**−58.94**	28.92	20.78	16.16	36.60	−26.73	−31.72
Kotli Sattian												
Arithmetic mean												
Horizontal (mm)	−29.32	−20.08	48.85	31.89	−55.96	**−170.70**	−0.22	159.53	79.42	7.77	−5.82	−45.36
Vertical (mm)	−34.29	−12.12	47.99	19.04	−38.47	**−191.68**	94.98	66.32	86.48	17.50	−18.43	−37.32
Std dev												
Horizontal (mm)	−24.30	−6.12	36.39	32.28	−11.78	**−98.16**	40.88	29.52	38.00	−0.19	−18.12	−18.42
Vertical (mm)	3.86	−49.94	45.94	26.86	−37.55	−35.49	19.11	−38.31	**92.08**	15.10	−28.35	−13.32

values of 2.10 and −3.93 are obtained for the maximum trend slopes, respectively, in March and April. These values show that the transition between 2 months is severe.

Trend polygon star concept method calculated monthly direction of horizontal (first-half duration) and vertical (second-half duration) projections, monthly amount changes (increasing or decreasing), and slope of total rainfall data for each station. With this analysis, it was possible to observe the maximum and minimum change amounts between the averages of two successive months according to the size of trend lengths and trend slopes. Trend polygon star concept arrows for each station were in I and III regions, showing the transition between two months for rainfall datasets using arithmetic mean and standard deviation. The highest transition was observed in August–September (A-S; highly increasing) and June–July (J-J; highly decreasing) between two months in all the stations

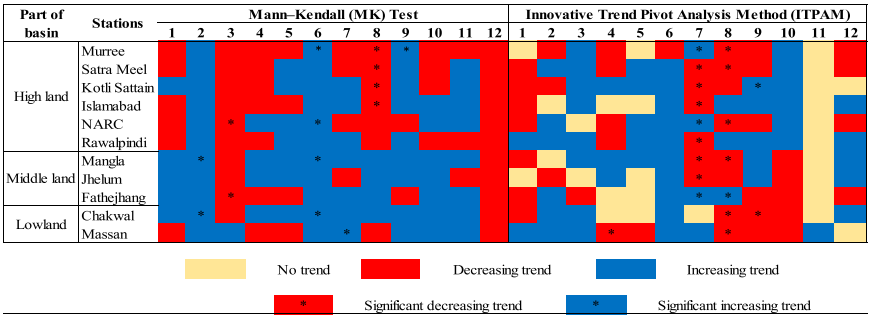

FIG. 7. Comparison of trend tests (MK and ITPAM) for total monthly rainfall data based on results from this study and from Hussain et al. (2021). The asterisk represents trend at $\alpha = 0.05$ level of significance.

based on the arithmetic mean. J-J is representing the highest transition in most of the stations under standard deviation. Four months (D-J, J-F, M-J, and J-J) of all stations showed significant transitions within region III (decreasing trend) under the arithmetic mean. Arrows showing transitions between other months (M-A, A-M, A-S, S-O, and O-N) are in region I (increasing trend). The standard deviation arrows showing the transition between both months are in the first three regions. Arrow direction in region II (IV) represents an increase (decrease) in the first (second) half time duration, and the longest arrow indicates the highest transition.

In this paper, monthly polygonal trends with risk graphs depict a clear picture of climate change effects in the Potohar region of Pakistan. Monsoonal months' (June, July, August, and September) rainfall of all stations shows a complex nature of behavior, and monthly distribution is uneven. There is a decreasing trend of rainfall in high land stations of Soan River basin, with a significant change between the first dataset and second dataset in July and August. It was also noted that monsoon rainfall is increasing in lowland stations, indicating a shifting pattern of monsoonal rainfall from highland to lowland areas of the Soan River basin. There exist both increasing and decreasing trends in different periods with evidence of seasonal variations that will cause irregular behavior in the water resources and agricultural sectors.

Acknowledgments. The authors acknowledge the Pakistan Meteorological Department (PMD) and Surface Water Hydrology Project–Water and Power Development Authority (SWHP-WAPDA) and Soil and Water Conservation Research Institute (SAWCRI) for the provision of rainfall data. All authors declare no conflict of interest.

Data availability statement. The data presented in this study are available on request.

REFERENCES

Achite, M., G. Ceribasi, A. I. Ceyhunlu, A. Wałęga, and T. Caloiero, 2021: The innovative polygon trend analysis (IPTA) as a simple qualitative method to detect changes in environment—Example detecting trends of the total monthly precipitation in semiarid area. *Sustainability*, **13**, 12674, https://doi.org/10.3390/su132212674.

Adnan, S., and K. Ullah, 2022: Long-term trends in climate parameters and multiple indices for drought monitoring over Pakistan. *Meteor. Atmos. Phys.*, **75** (4), 1–22, https://doi.org/10.1007/s00703-022-00908-3.

——, ——, and R. Ahmed, 2019: Variability in meteorological parameters and their impact on evapotranspiration in a humid zone of Pakistan. *Meteor. Appl.*, **27**, e1859, https://doi.org/10.1002/met.1859.

Ahmad, I., D. Tang, T. Wang, M. Wang, and B. Wagan, 2015: Precipitation trends over time using Mann-Kendall and Spearman's rho tests in Swat River Basin, Pakistan. *Adv. Meteor.*, **2015**, 431860, https://doi.org/10.1155/2015/431860.

Ahmed, K., S. Shahid, E. S. Chung, T. Ismail, and X. J. Wang, 2017: Spatial distribution of secular trends in annual and seasonal precipitation over Pakistan. *Climate Res.*, **74**, 95–107, https://doi.org/10.3354/cr01489.

Ahmed, N., G. Wang, M. J. Booij, G. Ceribasi, M. S. Bhat, A. I. Ceyhunlu, and A. Ahmed, 2022: Changes in monthly streamflow in the Hindukush–Karakoram–Himalaya Region of Pakistan using innovative polygon trend analysis. *Stochastic Environ. Res. Risk Assess.*, **36**, 811–830, https://doi.org/10.1007/s00477-021-02067-0.

Akçay, F., M. Kankal, and M. Şan, 2022: Innovative approaches to the trend assessment of streamflows in the eastern Black Sea basin, Turkey. *Hydrol. Sci. J.*, **67**, 222–247, https://doi.org/10.1080/02626667.2021.1998509.

Aktaş, B., 2020: Possible changes in some climate parameters and climate types in Konya depending on global warming. Kastamonu University Institute of Science Department of Sustainable Agriculture and Natural Plant Resources Rep.

Alashan, S., 2018: An improved version of innovative trend analyses. *Arab. J. Geosci.*, **11**, 50, https://doi.org/10.1007/s12517-018-3393-x.

Ali, S., B. Khalid, R. S. Kiani, R. Babar, S. Nasir, N. Rehman, M. Adnan, and M. A. Goheer, 2020: Spatio-temporal variability of summer monsoon onset over Pakistan. *Asia-Pac. J. Atmos. Sci.*, **56**, 147–172, https://doi.org/10.1007/s13143-019-00130-z.

Alifujiang, Y., J. Abuduwaili, B. Maihemuti, B. Emin, and M. Groll, 2020: Innovative trend analysis of precipitation in the lake Issyk-Kul Basin, Kyrgyzstan. *Atmosphere*, **11**, 332, https://doi.org/10.3390/atmos11040332.

Almazroui, M., Z. Şen, A. M. Mohorji, and M. Nazrul Islam, 2019: Impacts of climate change on water engineering structures in arid regions: Case studies in Turkey and Saudi Arabia. *Earth Syst. Environ.*, **3**, 43–57, https://doi.org/10.1007/s41748-018-0082-6.

Asmat, U., H. Athar, A. Nabeel, and M. Latif, 2018: An AOGCM based assessment of interseasonal variability in Pakistan. *Climate Dyn.*, **50**, 349–373, https://doi.org/10.1007/s00382-017-3614-0.

Bari, S. H., M. T. U. Rahman, M. A. Hoque, and M. M. Hussain, 2016: Analysis of seasonal and annual rainfall trends in the northern region of Bangladesh. *Atmos. Res.*, **176–177**, 148–158, https://doi.org/10.1016/j.atmosres.2016.02.008.

Birara, H., R. P. Pandey, and S. K. Mishra, 2018: Trend and variability analysis of rainfall and temperature in the Tana basin region, Ethiopia. *J. Water Climate Change*, **9**, 555–569, https://doi.org/10.2166/wcc.2018.080.

Bocheva, L., T. Marinova, P. Simeonov, and I. Gospodinov, 2009: Variability and trends of extreme precipitation events over Bulgaria (1961–2005). *Atmos. Res.*, **93**, 490–497, https://doi.org/10.1016/j.atmosres.2008.10.025.

Bradley, R. S., H. F. Diaz, J. K. Eischeid, P. D. Jones, P. M. Kelly, and C. M. Goodess, 1987: Precipitation Fluctuations over Northern Hemisphere land areas since the mid-19th century. *Science*, **237**, 171–175, https://doi.org/10.1126/science.237.4811.171.

Burn, D. H., 1994: Hydrologic effects of climatic change in west-central Canada. *J. Hydrol.*, **160**, 53–70, https://doi.org/10.1016/0022-1694(94)90033-7.

Ceribasi, G., and A. I. Ceyhunlu, 2021: Analysis of total monthly precipitation of Susurluk Basin in Turkey using innovative polygon trend analysis method. *J. Water Climate Change*, **12**, 1532–1543, https://doi.org/10.2166/wcc.2020.253.

——, ——, and N. Ahmed, 2021a: Innovative trend pivot analysis method (ITPAM): A case study for precipitation data of

Susurluk Basin in Turkey. *Acta Geophys.*, **69**, 1465–1480, https://doi.org/10.1007/s11600-021-00605-6.

——, ——, and ——, 2021b: Analysis of temperature data by using innovative polygon trend analysis and trend polygon star concept methods: A case study for Susurluk Basin, Turkey. *Acta Geophys.*, **69**, 1949–1961, https://doi.org/10.1007/s11600-021-00632-3.

Chang, X., Z. Xu, G. Zhao, T. Cheng, and S. Song, 2018: Spatial and temporal variations of precipitation during 1979–2015 in Jinan City, China. *J. Water Climate Change*, **9**, 540–554, https://doi.org/10.2166/wcc.2017.029.

Chattopadhyay, S., and D. R. Edwards, 2016: Long-term trend analysis of precipitation and air temperature for Kentucky, United States. *Climate*, **4**, 10, https://doi.org/10.3390/cli4010010.

Chaudhry, Q.-U.-Z., A. Mahmood, G. Rasul, and M. Afzaal, 2009: Climate change indicators of Pakistan. Pakistan Meteorological Department Tech. Rep. PMD-22/2009, 42 pp.

Dabanlı, İ., and Z. Şen, 2018: Classical and innovative-Şen trend assessment under climate change perspective. *Int. J. Global Warming*, **15**, 19–37, https://doi.org/10.1504/IJGW.2018.10006669.

Diaz, H. F., R. S. Bradley, and J. K. Eischeid, 1989: Precipitation fluctuations over global land areas since the late 1800's. *J. Geophys. Res.*, **94**, 1195, https://doi.org/10.1029/JD094iD01p01195.

Elouissi, A., Z. Şen, and M. Habi, 2016: Algerian rainfall innovative trend analysis and its implications to Macta watershed. *Arab. J. Geosci.*, **9**, 303, https://doi.org/10.1007/s12517-016-2325-x.

Güçlü, Y. S., 2018: Multiple Şen-innovative trend analyses and partial Mann-Kendall test. *J. Hydrol.*, **566**, 685–704, https://doi.org/10.1016/j.jhydrol.2018.09.034.

——, E. Şişman, and M. Ö. Yeleğen, 2018: Climate change and frequency-intensity-duration (FID) curves for Florya station, Istanbul. *J. Flood Risk Manag.*, **11**, S403–S418, https://doi.org/10.1111/jfr3.12229.

Hanif, M., A. H. Khan, and S. Adnan, 2013: Latitudinal precipitation characteristics and trends in Pakistan. *J. Hydrol.*, **492**, 266–272, https://doi.org/10.1016/j.jhydrol.2013.03.040.

Hırca, T., G. Eryılmaz Türkkan, and M. Niazkar, 2022: Applications of innovative polygonal trend analyses to precipitation series of eastern Black Sea Basin, Turkey. *Theor. Appl. Climatol.*, **147**, 651–667, https://doi.org/10.1007/s00704-021-03837-0.

Hossain, M. S., K. Roy, and D. K. Datta, 2014: Spatial and temporal variability of rainfall over the south-west coast of Bangladesh. *Climate*, **2**, 28–46, https://doi.org/10.3390/cli2020028.

Hussain, F., G. Nabi, and M. W. Boota, 2015: Rainfall trend analysis by using the Mann-Kendall test & Sen's slope estimates: A case study of District Chakwal rain gage, Barani area. *Sci. Int.*, **27**, 3159–3165.

——, ——, and R.-S. Wu, 2021: Spatiotemporal rainfall distribution of Soan River basin, Pothwar region, Pakistan. *Adv. Meteor.*, **2021**, 665673, https://doi.org/10.1155/2021/6656732.

Hussain, M. S., and S. Lee, 2014: Long-term variability and changes of the precipitation regime in Pakistan. *Asia-Pac. J. Atmos. Sci.*, **50**, 271–282, https://doi.org/10.1007/s13143-014-0015-8.

IPCC, 2007: *Climate Change 2007: Impacts, Adaptation, and Vulnerability*. Cambridge University Press, 976 pp., https://www.ipcc.ch/pdf/assessment-report/ar4/wg2/ar4_wg2_full_report.pdf.

——, 2021: Summary for policymakers. *Climate Change 2021: The Physical Science Basis*, V. Masson-Delmotte et al., Eds., Cambridge University Press, 32 pp., https://www.ipcc.ch/report/ar6/wg1/downloads/report/IPCC_AR6_WGI_SPM.pdf.

Jones, J. R., J. S. Schwartz, K. N. Ellis, J. M. Hathaway, and C. M. Jawdy, 2015: Temporal variability of precipitation in the upper Tennessee valley. *J. Hydrol. Reg. Stud.*, **3**, 125–138, https://doi.org/10.1016/j.ejrh.2014.10.006.

Kabanda, T., 2018: Long-term rainfall trends over the Tanzania coast. *Atmosphere*, **9**, 155, https://doi.org/10.3390/atmos9040155.

Kendall, M. G., 1975: *Rank Correlation Methods*. Charles Griffin, 202 pp.

Khatiwada, K. R., J. Panthi, M. L. Shrestha, and S. Nepal, 2016: Hydro-climatic variability in the Karnali River basin of Nepal Himalaya. *Climate*, **4**, 17, https://doi.org/10.3390/cli4020017.

Korhonen, J., and E. Kuusisto, 2010: Long-term changes in the discharge regime in Finland. *Hydrol. Res.*, **41**, 3–4, https://doi.org/10.2166/nh.2010.112.

Kyselý, J., 2009: Trends in heavy precipitation in the Czech Republic over 1961-2005. *Int. J. Climatol.*, **29**, 1745–1758, https://doi.org/10.1002/joc.1784.

Maheras, P., 1988: Changes in precipitation conditions in the western Mediterranean over the last century. *J. Climatol.*, **8**, 179–189, https://doi.org/10.1002/joc.3370080205.

Malik, A., and A. Kumar, 2020: Spatio-temporal trend analysis of rainfall using parametric and non-parametric tests: Case study in Uttarakhand, India. *Theor. Appl. Climatol.*, **140**, 183–207, https://doi.org/10.1007/s00704-019-03080-8.

Mann, H. B., 1945: Nonparametric tests against trend. *Econometrica*, **13**, 245–259, https://doi.org/10.2307/1907187.

Mitchell, J. M., B. Dzerdzeevkii, H. Flohn, W. L. Hofmeyr, H. H. Lamb, K. N. Rao, and C. C. Wallén, 1966: Climatic change. WMO Tech. Note 195, 79 pp., https://library.wmo.int/doc_num.php?explnum_id=865.

Mohorji, A. M., Z. Şen, and M. Almazroui, 2017: Trend analyses revision and global monthly temperature innovative multiduration analysis. *Earth Syst. Environ.*, **1**, 9, https://doi.org/10.1007/s41748-017-0014-x.

Nabi, G., F. Hussain, R.-S. Wu, V. Nangia, and R. Bibi, 2020: Micro-watershed management for erosion control using soil and water conservation structures and SWAT modeling. *Water*, **12**, 1439, https://doi.org/10.3390/w12051439.

Naheed, G., D. H. Kazmi, and G. Rasul, 2013: Seasonal variation of rainy days in Pakistan. *Pak. J. Meteor.*, **9**, 9–13.

Nawaz, Z., X. Li, Y. Chen, Y. Guo, X. Wang, and N. Nawaz, 2019: Temporal and spatial characteristics of precipitation and temperature in Punjab, Pakistan. *Water*, **11**, 1916, https://doi.org/10.3390/w11091916.

Phuong, D. N. D., V. T. Linh, T. T. Nhat, H. M. Dung, and N. K. Loi, 2019: Spatiotemporal variability of annual and seasonal rainfall time series in Ho Chi Minh city, Vietnam. *J. Water Climate Change*, **10**, 658–670, https://doi.org/10.2166/wcc.2018.115.

Reihan, A., J. Kriauciuniene, D. Meilutyte-Barauskiene, and T. Kolcova, 2012: Temporal variation of spring flood in rivers of the Baltic States. *Hydrol. Res.*, **43**, 301–314, https://doi.org/10.2166/nh.2012.141.

Rodriguez-Puebla, C., A. H. Encinas, S. Nieto, and J. Garmendia, 1998: Spatial and temporal patterns of annual precipitation variability over the Iberian Peninsula. *Int. J. Climatol.*, **18**, 299–316, https://doi.org/10.1002/(SICI)1097-0088(19980315)18:3<299::AID-JOC247>3.0.CO;2-L.

Safdar, F., M. F. Khokhar, M. Arshad, and I. H. Adil, 2019: Climate change indicators and spatiotemporal shift in monsoon patterns in Pakistan. *Adv. Meteor.*, **2019**, 1–14, https://doi.org/10.1155/2019/8281201.

Salma, S., S. Rehman, and M. A. Shah, 2012: Rainfall trends in different climate zones of Pakistan. *Pak. J. Meteor.*, **9**, 37–47.

Şan, M., F. Akçay, N. T. T. Linh, M. Kankal, and Q. B. Pham, 2021: Innovative and polygonal trend analyses applications for rainfall data in Vietnam. *Theor. Appl. Climatol.*, **144**, 809–822, https://doi.org/10.1007/s00704-021-03574-4.

Sayemuzzaman, M., and M. K. Jha, 2014: Seasonal and annual precipitation time series trend analysis in North Carolina, United States. *Atmos. Res.*, **137**, 183–194, https://doi.org/10.1016/j.atmosres.2013.10.012.

Sen, P. K., 1968: Estimates of the regression coefficient based on Kendall's tau. *J. Amer. Stat. Assoc.*, **63**, 1379–1389, https://doi.org/10.1080/01621459.1968.10480934.

Şen, Z., 2012: Innovative trend analysis methodology. *J. Hydrol. Eng.*, **17**, 1042–1046, https://doi.org/10.1061/(ASCE)HE.1943-5584.0000556.

——, 2014: Trend identification simulation and application. *J. Hydrol. Eng.*, **19**, 635–642, https://doi.org/10.1061/(ASCE)HE.1943-5584.0000811.

——, 2017a: *Innovative Trend Methodologies in Science and Engineering*. Springer, 349 pp.

——, 2017b: Innovative trend significance test and applications. *Theor. Appl. Climatol.*, **127**, 939–947, https://doi.org/10.1007/s00704-015-1681-x.

——, 2021: Conceptual monthly trend polygon methodology and climate change assessments. *Hydrol. Sci. J.*, **66**, 503–512, https://doi.org/10.1080/02626667.2021.1881099.

——, E. Şişman, and I. Dabanli, 2019: Innovative polygon trend analysis (IPTA) and applications. *J. Hydrol.*, **575**, 202–210, https://doi.org/10.1016/j.jhydrol.2019.05.028.

Singh, R. N., S. Sah, B. Das, S. Potekar, A. Chaudhary, and H. Pathak, 2021: Innovative trend analysis of spatio-temporal variations of rainfall in India during 1901–2019. *Theor. Appl. Climatol.*, **145**, 821–838, https://doi.org/10.1007/s00704-021-03657-2.

Sonali, P., and D. Nagesh Kumar, 2013: Review of trend detection methods and their application to detect temperature changes in India. *J. Hydrol.*, **476**, 212–227, https://doi.org/10.1016/j.jhydrol.2012.10.034.

Swain, S., M. Verma, and M. K. Verma, 2015: Statistical trend analysis of monthly rainfall for Raipur District, Chhattisgarh. *Int. J. Adv. Eng. Res. Stud.*, **2015**, 87–89.

Tabari, H., B. S. Somee, and M. R. Zadeh, 2011: Testing for long-term trends in climatic variables in Iran. *Atmos. Res.*, **100**, 132–140, https://doi.org/10.1016/j.atmosres.2011.01.005.

——, M. T. Taye, C. Onyutha, and P. Willems, 2017: Decadal analysis of river flow extremes using quantile-based approaches. *Water Resour. Manage.*, **31**, 3371–3387, https://doi.org/10.1007/s11269-017-1673-y.

Theil, H., 2011: A rank-invariant method of linear and polynomial regression analysis. *Theoret. Appl. Econom.*, **23**, 345–381, https://doi.org/10.1007/978-94-011-2546-8_20.

Türkeş, M., T. Koç, and F. Sariş, 2009: Spatiotemporal variability of precipitation total series over Turkey. *Int. J. Climatol.*, **29**, 1056–1074, https://doi.org/10.1002/joc.1768.

Wang, Y., Y. Xu, H. Tabari, J. Wang, Q. Wang, S. Song, and Z. Hu, 2020: Innovative trend analysis of annual and seasonal rainfall in the Yangtze River delta, eastern China. *Atmos. Res.*, **231**, 104673, https://doi.org/10.1016/j.atmosres.2019.104673.

Wilson, D., H. Hisdal, and D. Lawrence, 2010: Has streamflow changed in the Nordic countries?—Recent trends and comparisons to hydrological projections. *J. Hydrol.*, **394** (3–4), 334–346, https://doi.org/10.1016/j.jhydrol.2010.09.010.

Wu, H., and H. Qian, 2017: Innovative trend analysis of annual and seasonal rainfall and extreme values in Shaanxi, China, since the 1950s. *Int. J. Climatol.*, **37**, 2582–2592, https://doi.org/10.1002/joc.4866.

Yu, B., and D. T. Neil, 1993: Long-term variations in regional rainfall in the south-west of Western Australia and the difference between average and high intensity rainfalls. *Int. J. Climatol.*, **13**, 77–88, https://doi.org/10.1002/joc.3370130106.

Yu, Y.-S., S. Zou, and D. Whittemore, 1993: Non-parametric trend analysis of water quality data of rivers in Kansas. *J. Hydrol.*, **150**, 61–80, https://doi.org/10.1016/0022-1694(93)90156-4.

Zhang, A., C. Zheng, S. Wang, and Y. Yao, 2015: Analysis of streamflow variations in the Heihe River basin, northwest China: Trends, abrupt changes, driving factors and ecological influences. *J. Hydrol. Reg. Stud.*, **3**, 106–124, https://doi.org/10.1016/j.ejrh.2014.10.005.